UV-induced transformation of 2,3-dibromo-5,6-dimethyl-1,4-benzoquinone in water and treated wastewater

(Article begins on next page)

05 May 2024

UV-induced transformation of 2,3-dibromo-5,6-dimethyl-1,4-benzoquinone in water and treated wastewater

Efstathia Kourounioti[a], Elefteria Psillakis[a,]* and Davide Vione[b,]*

[a] Laboratory of Aquatic Chemistry, School of Environmental Engineering, Technical University of Crete, GR-73100, Chania, Crete, Greece
[b] Dipartimento di Chimica, Università degli Studi di Torino, Via P. Giuria 5, I-10125, Torino, Italy

* Corresponding authors e-mails:
elia@enveng.tuc.gr (E.Psillakis)
davide.vione@unito.it (D. Vione)

Abstract

In this work, we investigate the photolysis behavior of 2,3-dibromo-5,6-dimethyl-1,4-benzoquinone (DDBQ), the only dibrominated benzoquinone detected in treated water so far. DDBQ solutions prepared in ultra-pure water were exposed to UV radiation centered at 254 nm (UV$_{254}$), and the photolysis of the parent compound was monitored together with by-product formation. The DDBQ pseudo-first order photolysis rate constants decreased when increasing the initial DDBQ concentration, and this behavior was caused by saturation of absorption. The photodegradation kinetics was found not to depend on pH and 1-butanol addition, but was affected by humic acids and components that occur in both natural waters and treated wastewater. For the first time with this class of compounds, photolysis studies were also performed using natural and treated wastewater matrices, where photodegradation was always found to proceed significantly slower than in ultra-pure water. The implications for the radiation dose that is required to reach a given treatment target are discussed, and a numerical approach by which to foresee the extent of degradation inhibition is provided that should be taken into account when planning the UV$_{254}$ treatment of DDBQ. The phototransformation of DDBQ yielded hydroxyderivatives, most likely via a debromination-hydroxylation pathway. *In-silico* toxicity screening suggested that the transformation of DDBQ into the detected hydroxyderivatives would not eliminate toxicity. Although the monohydroxylated derivative underwent relatively fast transformation, the dihydroxylated compound was found to accumulate during irradiation. As a compromise, the irradiation conditions that produce over 90% degradation of DDBQ in the studied samples, and at the same time keep by-product formation low are discussed.

Keywords: Disinfection by-products; dibrominated benzoquinone; photolysis; natural water; treated wastewater; in-silico toxicity estimates.

1. Introduction

Disinfection of water is essential to inactivate pathogens and has saved millions of lives from infectious diseases. However, this type of treatment can lead to the unintentional production of disinfection by-products (DBP) from the reactions of disinfectants with organic matter naturally present in water (Li et al., 2015). According to epidemiological studies, DBP exposure is potentially associated with increased risk in bladder cancer and inconsistently associated with adverse reproductive outcomes (Wang et al, 2016). For this reason, the most abundant DBPs including trihalomethanes (THMs) and haloacetic acids (HAAs) are now regulated by law, though more than 600 DBPs have been reported (Wang et al, 2016).

In 2010, halobenzoquinones (HBQs) were identified as an emerging class of DBPs in drinking water (Zhao et al., 2010, Qin et al., 2010). The presence of 2,6-dichloro-1,4-benzoquinone (2,6-DCBQ), 2,6-dichloro-3-methyl-1,4-benzoquinone (DCMBQ), 2,3,6-trichloro-1,4-benzoquinone (TriCBQ), and 2,6-dibromo-1,4-benzoquinone (2,6-DBBQ) at ng L^{-1} concentration level was initially confirmed in drinking water disinfected with chlorination (Zhao et al., 2010) or with chloramines plus UV irradiation (Zhao et el. 2010). A subsequent report expanded the studies and included another four target HBQs: 2,5-DBBQ, 2,3-dibromo-5,6-dimethyl-1,4-benzoquinone (DDBQ) and two TetraBBQ isomers (Zhao et al., 2012). Although none of these newly screened HBQs was identified in the examined drinking water samples, the presence of DDBQ was later confirmed in samples from swimming-pool water at concentrations between 0.6-0.7 ng L^{-1} (Wang et al., 2013). The same study reported higher occurrence frequency and concentrations of HBQs in recreational water compared to drinking water. This finding was related to the higher dissolved organic carbon (DOC), higher doses of chlorine and higher temperature that promoted the formation of HBQs in the pools (Wang et al., 2013).

The presence of electron-withdrawing groups in benzoquinones increases cytotoxicity, with brominated derivatives showing higher levels of cytotoxicity and genotoxicity than their chlorinated analogues (Anichina et al., 2010; Bull et al. 2011). Accordingly, despite the relatively low concentrations of brominated BQs in water samples, the suggested toxicity levels set a clear need for additional data on their environmental fate. In particular, it is important to provide more evidence on how brominated BQs may be removed or transformed after exposing them to UV irradiation, as part of a UV disinfection treatment process or naturally occurring reactions. To this end, a previous study has investigated the photochemical transformation of DBBQ and three chlorinated BQs under UV_{254} (Qian et al., 2013). The UV-induced DBBQ removal rates were found

to be similar in ultra-pure and tap water samples, and the major reported photoproduct was 3-hydroxy-DBBQ (OHDBBQ) (Qian et al., 2013).

The focus of the present work was to investigate the photolysis behavior of DDBQ, the only dibrominated benzoquinone detected in disinfected water samples. Water samples spiked with DDBQ were irradiated by UV_{254} and degradation rates and by-product formation were recorded. The effect of different parameters on the photolysis rates was studied in separate sets of experiments, and the results were used for the modeling of the UV_{254}-based treatment process. In this way it was possible to get insight into the impact of several parameters such as water matrix composition, substrate and (if relevant) additives concentration, next to determine the conditions in which the treatment process can be most effective (Gligorovski et al., 2015; Lanzafame et al., 2017). Finally, this is the first report that investigates the effect of the water matrix on HBQ photolysis fate by using both natural and treated wastewater samples.

2. Experimental

2.1. Chemicals and samples

DDBQ was 99.5% pure and was purchased from Sigma-Aldrich (Steinheim, Germany). All organic solvents used were of pesticide grade and were obtained from Sigma-Aldrich, with the exception of 1-butanol that was purchased from Riedel-de Haën (Seelze, Germany). Analytical grade formic acid, humic acid and potassium nitrate were supplied by Fluka Chemie GmbH (Bucks, Switzerland). When stated in the text, aqueous solutions of hydrochloric acid or sodium hydroxide (Fluka Chemie GmbH) were used to adjust the pH. Ultra-pure water was prepared by using an EASYpure RF water purification system supplied by Barnstead/Thermolyne Corporation (Dubuque, IA, USA). Aqueous working standards were prepared daily from a methanolic stock solution containing 10 g L^{-1} of DDBQ. The matrix effect on DDBQ photolysis was studied using: (i) freshwater sampled from the river Koiliaris at Kyani Akti (Kalyves, Crete, Greece); (ii) seawater sampled near the beach of Kyani Akti (Kalyves, Crete, Greece), and (iii) secondary treated wastewater effluent (WWTP Effluent) from the municipal wastewater treatment plant of Chania (Crete, Greece), serving approximately 70,000 inhabitants. The composition of the three sample types is given in Table S1 in the Supplementary Material. Samples were collected the day before conducting the photo-experiments and were stored in the dark at 4 °C. All samples were initially analyzed and found free of DDBQ.

2.2. Photolysis experiments in aqueous solution

A home-made laboratory photoreactor (28 cm × 28 cm × 28 cm) was used for all photolysis experiments. The photoreactor was equipped with two 8 W low-pressure mercury lamps (Philips TUV 8W G8 T5), each mounted on opposing sidewall of the photoreactor and having a strong emission line at 254 nm. The distance between each lamp and the quartz vial used in the experiments was 13 cm. The rate of the incident UV light intensity entering the solution (I_o, given in E L^{-1} s^{-1}, where E = Einstein) was determined to be I_o = (1.65± 0.06)×10^{-5} E L^{-1} s^{-1} using H_2O_2 as a chemical actinometer (see the Supplementary Material for further details) (Beltrán et al. 1995). The concentration of the aqueous H_2O_2 solution (0.15 M) was sufficiently high to assume that the actinometer absorbed all incident light and that the direct photolysis of the reactant followed zero-order kinetics (Beltrán et al. 1995, Schwarzenbach et al. 2003).

In all photolysis experiments, 5 mL of a DDBQ aqueous solution at a known concentration level was introduced in a tailor-made quartz vial (2.0 cm outer diameter × 4.8 cm height). It is noted, that photolysis was found to be a first-order reaction and therefore independent of the initial concentration. For this reason, tested concentrations were chosen so that the samples could be analyzed directly without preconcentration, thereby avoiding variation caused by the pretreatment. The vial containing the spiked water solution was then capped and submitted to UV irradiation for a preset time. The inner diameter of the quartz vial (1.8 cm) was used as the optical path length of radiation. After UV-exposure, samples were acidified to contain 0.25% v/v formic acid and were used for liquid chromatographic (LC) analysis without any pretreatment step. The addition of formic acid was previously found to effectively stabilize halobenzoquinones in water, as well as improve their ionization for mass spectrometry (MS) analysis (Zhao, 2010). Dark tests were run in parallel by placing the spiked water samples inside the photoreactor with the lamps switched off, so as to ensure that any decrease in the analytical signal was due to the action of photons alone. All experiments were run at least in duplicates.

2.3. Analytical methods

The absorbance of natural and treated wastewater samples at 254 nm was measured using a single-beam UV-visible spectrophotometer (UVmini-240, Shimadzu, Tokyo Japan), equipped with quartz cuvettes having a 1-cm optical path length.

All analyses on DDBQ and its transformation products were carried out using an Agilent 1200 Series high-performance liquid chromatography (HPLC) system equipped with a binary pump, autosampler, degasser and thermostated column compartment coupled to a diode array detector (DAD), and an Agilent 6110 single quadrupole LC-MS system equipped with a multimode ionization source. For analysis, 50 μL of the sample were added in 100 μL polypropylene inserts placed in 2 mL polypropylene autosampler vials equipped with caps, all purchased from Agilent (Palo Alto, USA). A Thermo-Electron Betasil C18 column (Waltham, MA, USA) of dimensions 2.1 mm ID × 100 mm length and 5 μm particle size was used for separation. The mobile phase consisted of solvent (A) water containing 0.25% formic acid and (B) methanol containing 0.25% formic acid. The LC gradient method used was 60% B for the first 1 min, then linearly increased to 90% B in 20 min where it was held for 4 min, followed by a 2 min ramp to 60% B where it was held for the rest of the analysis. The flow rate of the mobile phase was 200 μL min^{-1} and the total analysis time was 35 min. The MS conditions were: drying gas flow, 5 L min^{-1}; drying gas temperature, 350 °C; nebulizer pressure, 20 psi; collector capillary voltage, 2.0 kV; fragmentor voltage, 70 V; scan range (m/z) of 100-500 amu. The mass spectrometry data were recorded using the negative electrospray ionization (ESI) mode. The DAD signals were used at all times for monitoring DDBQ and its transformation products. Mass spectrometry was used to identify the eluting peaks. QA/QC procedures ensured that the system was operating within acceptable limits and that the method's performance was conforming. These procedures included analyzing a calibration standard for each set of photolysis experiments as a calibration check. QC samples consisted of running a method blank and laboratory control samples in each analytical batch. Method blank samples consisted of water containing 0.25% formic acid run in parallel to exclude contamination of the analytical instrumentation during analysis. The effect of the matrix on method performance (precision and accuracy) was initially evaluated for every synthetic, natural or treated wastewater matrix tested. Matrix spike and matrix spike duplicate aliquots were routinely analyzed and were used as laboratory control samples.

2.4. Kinetic Data Treatment

The DDBQ time trends were fitted with exponential equations of the form $C_{DDBQ} = C_{o,DDBQ} \exp(-k_{DDBQ} t)$, where C_{DDBQ} is the concentration of DDBQ at the time t, $C_{o,DDBQ}$ the initial concentration, and k_{DDBQ} the first-order degradation rate constant. The initial degradation rate of DDBQ was $R_{DDBQ}^{o} = k_{DDBQ} C_{o,DDBQ}$.

2.5. In-silico Toxicity Estimates

Acute-toxicity parameters (LC_{50} and EC_{50}) and chronic toxicity values (ChV) to aquatic organisms were assessed by using the ECOSAR V2.0 software [Ecological Structure Activity Relationships (ECOSAR) Class Program], developed by the U.S. Environmental Protection Agency (EPA) and freely available (https://www.epa.gov/tsca-screening-tools/ecological-structure-activity-relationships-ecosar-predictive-model; Mayo-Bean et al., 2012). The software computes toxicity parameters towards ecologically relevant freshwater organisms such as fish, crustaceans (daphnid) and green algae. The toxicity endpoint parameters for two different compounds can be considered as significantly different if the relevant values (LC_{50}, EC_{50} or ChV) differ by at least an order of magnitude. Several previous studies have used the ECOSAR software to predict the aquatic toxicity of chemicals (Reuschenbach et al., 2008; Frank et al., 2010; Ortiz de García et al., 2014).

3. Results and Discussion

3.1. Photodegradation kinetics of DDBQ

In a first series of experiments, DDBQ was irradiated at different initial concentration values in the range of 10-50 mg L^{-1} (*i.e.*, 34-170 µmol L^{-1}). Figure S2 shows the respective normalized concentration-time profiles, from which the apparent rate constants (k_{DDBQ}) could be computed assuming that photodegradation follows a pseudo-first order rate expression. The k_{DDBQ} took values of 0.1963 (r^2 = 0.9990), 0.1395 (r^2 = 0.9911) and 0.0935 (r^2 = 0.9963) min^{-1} (r^2 is the regression coefficient) at, respectively, 10, 25 and 50 mg L^{-1} initial DDBQ concentration ($C_{o,DDBQ}$). The fact that k_{DDBQ} decreased with increasing $C_{o,DDBQ}$ implied that the reaction kinetics did not follow a true first order (in which case the rate constant would be independent of the DDBQ concentration) and shifted towards zeroth order at high $C_{o,DDBQ}$ values.

The initial DDBQ photodegradation rate ($R^o_{DDBQ} = k_{DDBQ} C_{o,DDBQ}$) had an exponential increase with plateau as $C_{o,DDBQ}$ increased (Figure 1). In a direct photolysis process such kind of behavior is usually caused by saturation of absorption and, in this case, the initial degradation rate can be described by the following trend (Braslavsky, 2007):

7

$$R^O_{DDBQ} = \Phi_{DDBQ} I_o [1 - \exp(-2.303\ L\ \varepsilon_{DDBQ}\ C_{o,DDBQ})] \tag{1}$$

where Φ_{DDBQ} is the direct photolysis quantum yield of DDBQ, $I_o = (1.65 \pm 0.06) \times 10^{-5}$ E L^{-1} s^{-1} the incident UV light intensity, ε_{DDBQ} (3380 M^{-1} cm^{-1}) the molar absorption coefficient of DDBQ at 254 nm, and L (1.8 cm) the optical path length of radiation inside the irradiated solution. The fit of the experimental data with Eq. 1 gave an excellent agreement as shown in Figure 1, and the product $L\ \varepsilon_{DDBQ} = (5.9 \pm 0.3) \times 10^3$ M^{-1} that was derived from the fit matched very well the experimental datum (6050 M^{-1}) obtained by spectrophotometry. This means that absorption saturation was the cause of the plateau trend. Moreover, by assuming $I_o = (1.65 \pm 0.06) \times 10^{-5}$ E L^{-1} s^{-1}, the fit yielded $\Phi_{DDBQ} = 0.0178 \pm 0.0003$ (σ-level uncertainty). This quantum yield value is intermediate between those found for a series of halobenzoquinones (mostly chlorinated) and their hydroxyderivatives in a previous study (Qian et al., 2013).
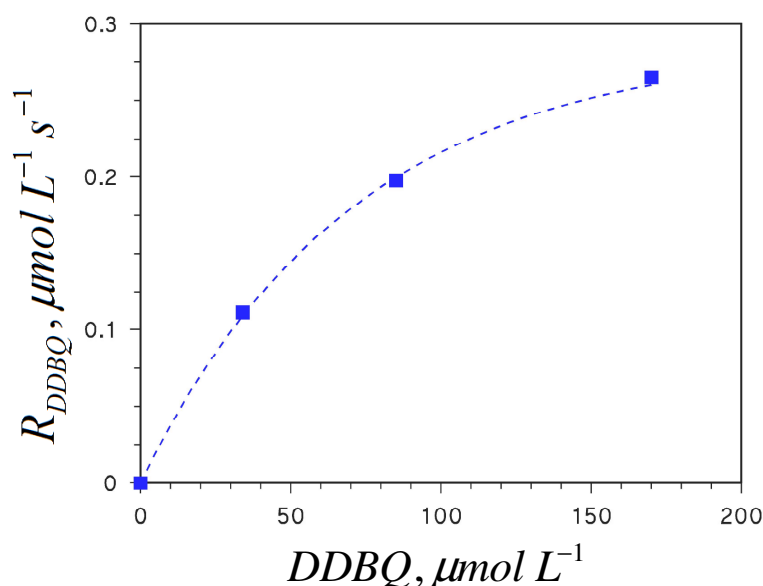

Figure 1. DDBQ initial photodegradation rate (R_{DDBQ}) in ultra-pure water under UV$_{254}$ irradiation, as a function of the initial DDBQ concentration. The dashed curve represents the data fit with Eq. (1).

The effect of pH on the photolysis of DDBQ was then investigated. The results showed that pH values of the irradiated solution in the range 3-9 had almost no effect on the photodegradation of DDBQ (Figure S3). Although these results were expected for a compound that does not undergo acid-base equilibrium, they were essential to confirm that the photolytical behavior of DDBQ for

different pH values remained constant and that DDBQ hydrolysis was negligible compared to photolysis. To this end, TetraCBQ has been found to undergo two-step hydrolysis under neutral or alkaline conditions (Veltistas et al., 1994; Sarr et al., 1995; Wang et al., 2016). In a separate set of experiments the effect of 1-butanol was investigated. 1-Butanol is a very effective radical scavenger that reacts preferentially with hydroxyl radicals, and may thus retard or even quench the degradation of parent organic compounds (Javier Benitez et al., 2013). Here, the addition of 1-butanol at 10 mmol L^{-1} concentration had practically no effect on the kinetics of the DDBQ direct photolysis (Figure S4), thereby excluding the involvement of hydroxyl radicals in the reaction.

In general, humic acids (HA) may act as photosensitizers by generating a range of reactive transient species including triplet states and $^1O_2$. However, the results shown in Figure 2 reveal that the addition of HA significantly inhibited the photodegradation of DDBQ. This is most likely due to the screening of radiation operated by HA, which decreases the photon flux absorbed by DDBQ and as such inhibits direct photolysis. The extent of radiation screening by HA on DDBQ can be assessed quite easily, by considering the photon fluxes (*pf*) absorbed by DDBQ in the absence and in the presence of HA. The ratio, ρ, among the two photon fluxes can be expressed by the following equation (Braslavsky, 2007):

$$\rho = \frac{pf_{DDBQ\,alone}}{pf_{DDBQ,HA}} = \frac{A_{DDBQ} + A_{HA}}{A_{DDBQ}} \times \frac{1 - \exp(-2.303\,A_{DDBQ})}{1 - \exp[-2.303(A_{HA} + A_{DDBQ})]} \qquad (4)$$

where A_{HA} (1.0 at 254 nm) is the absorbance of HA in the irradiated system. It is noted that the A_{HA} value was close to that of DDBQ ($A_{DDBQ} \sim 1$). One gets $\rho = 1.8$, which means that HA almost halved the absorption of radiation by DDBQ. The value of ρ thus obtained can be compared with the ratio ρ' of the experimental first-order rate constants of DDBQ without and with HA, $\rho' = k_{DDBQ\,alone}(k_{DDBQ,HA})^{-1} = 6.2$. The comparison between ρ and ρ' suggests that HA inhibits the photodegradation of DDBQ to a higher extent than is expected by mere competition for irradiance (i.e., HA inhibits DDBQ photodegradation by over 6 times, compared to ~ 2 times as expected by mere light screening). It can thus be assumed that HA are also able to decrease the photolysis quantum yield of DDBQ, by acting either as anti-oxidants or as excited-state scavengers. Both phenomena have been reported previously (Canonica and Laubscher, 2008; Vione et al., 2010). The apparent photolysis quantum yield in the studied experimental system can be calculated as

$\Phi^a_{DDBQ} = \Phi_{DDBQ}\rho/\rho'$. In the case of 35 mg L^{-1} HA as used in this work, the apparent photolysis quantum yield was $\Phi^a_{DDBQ} = 0.0052$, instead of $\Phi_{DDBQ} = 0.0178$ observed with DDBQ alone.
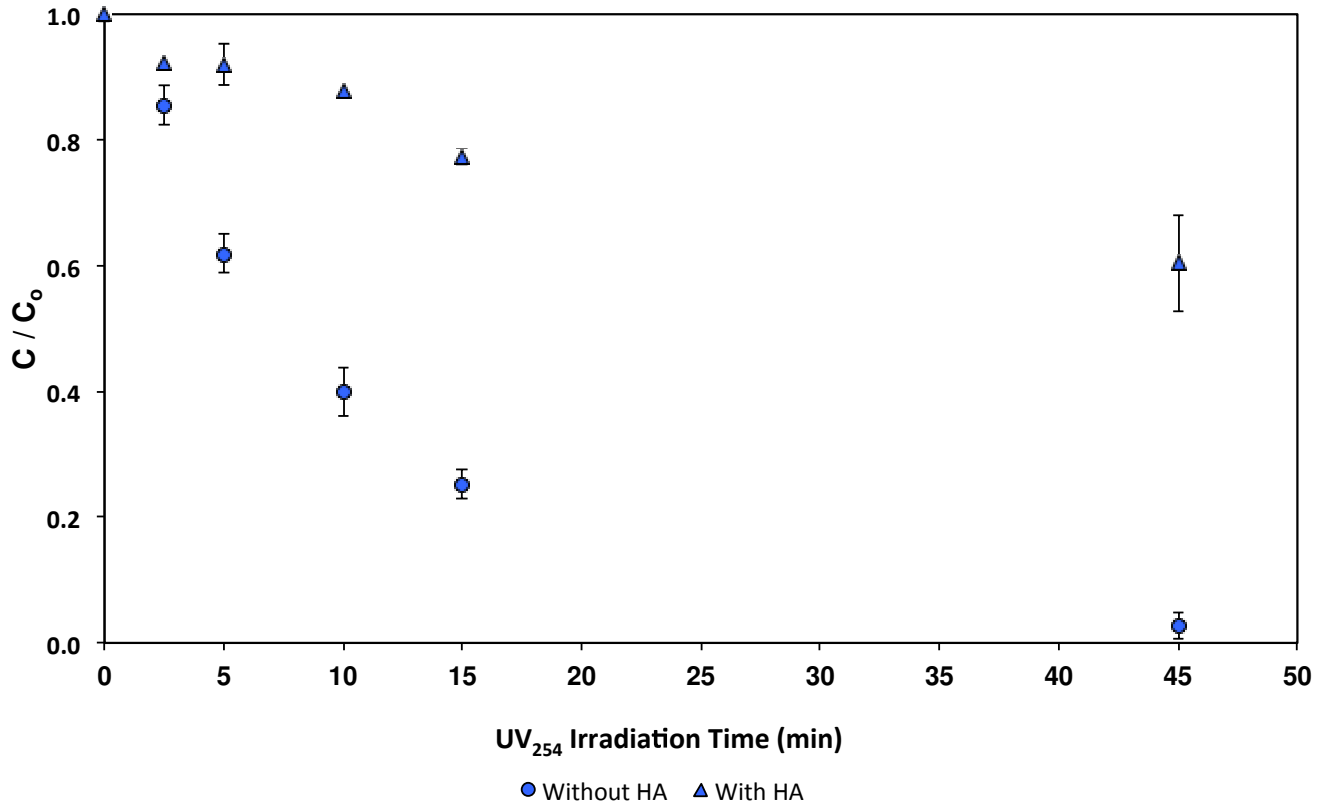

Figure 2. Photolysis of DDBQ in ultra-pure water and in the presence of humic acids (HA; 35 mg L^{-1}) under UV$_{254}$ irradiation. Initial DDBQ concentration for both experiments: C$_o$ = 50 mg L^{-1}.

The photodegradation of DDBQ was also studied in various natural and treated wastewater matrices (river water, seawater, effluent wastewater), and compared with the behavior of DDBQ in ultra-pure water (see Figure 3).
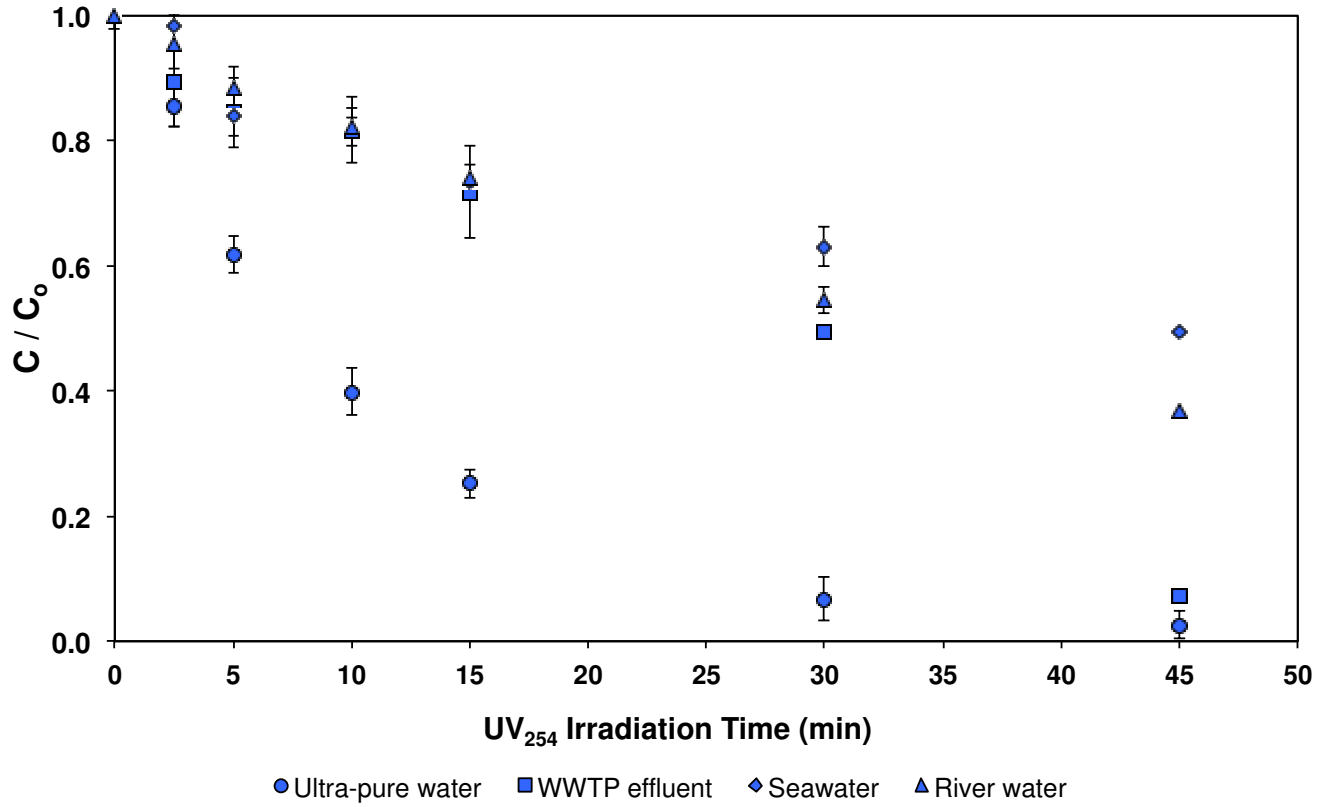
Figure 3. Photolysis of 50 mg L^{-1} (C$_o$) DDBQ solutions in ultra-pure water, river water, seawater and effluent wastewater (WWTP), under UV$_{254}$ irradiation.

It can be seen from the experimental data that the kinetics of DDBQ direct photolysis were slower in all investigated water matrices compared to ultra-pure water. It is again possible to test the hypothesis that the inhibition of photodegradation was caused by competition for lamp irradiance between DDBQ and the natural-water components. In an analogous way as already done for HA (Eq. (4)), it is possible to get quantitative insight into the irradiance competition between DDBQ and the natural and treated wastewater matrices studied here. To this end, Eq. (4) can be modified as follows:

$$\rho = \frac{pf_{DDBQ\,alone}}{pf_{DDBQ,W}} = \frac{A_{DDBQ} + A_W}{A_{DDBQ}} \times \frac{1 - \exp(-2.303\,A_{DDBQ})}{1 - \exp[-2.303(A_W + A_{DDBQ})]} \qquad (5)$$

where ρ is the ratio of the radiation absorption intensity of DDBQ in ultra-pure water and in the studied water matrix W (note that it was again $A_{\text{DDBQ}} \sim 1$), and A_{W} is the absorbance of the natural or treated wastewater matrix in the photoreactor. The calculated ρ value can again be compared with the experimental datum $\rho' = k_{DDBQ\,alone}(k_{DDBQ,W})^{-1}$, which represents the ratio between the degradation rate constants of DDBQ in ultra-pure water and in the studied water matrix.

Table 1 reports the values of A_{W} (absorbance at 254 nm inside the irradiated photoreactor) for the studied river-, sea- and wastewater samples, as well as the values of ρ, ρ' and $\Phi^a_{DDBQ} = \Phi_{DDBQ}\rho / \rho'$. In all cases, it is evident that the studied water matrices inhibited DDBQ photodegradation, to a higher extent ($\rho' > \rho$) than could be expected from a mere light-screening effect. Therefore, a decrease of the direct photolysis quantum yield ($\Phi^a_{DDBQ} < \Phi_{DDBQ}$) has to be assumed. For all the investigated water matrices we found $\Phi^a_{DDBQ} \sim 0.004$, which is also close to the Φ^a_{DDBQ} value observed with HA. Interestingly, seawater exhibited a similar Φ^a_{DDBQ} value as freshwater and wastewater, implying that sea salts might not affect the direct photolysis of DDBQ.

These findings suggest that $\Phi^a_{DDBQ} = 0.004$ provides a convenient description of the photodegradation behavior of DDBQ in the studied natural or treated wastewater samples under UV_{254} irradiation. By making reasonable assumptions, it is possible to get insight into the extent by which the UV_{254} photodegradation of DDBQ in real water may deviate from the results observed in ultra-pure water systems. To do this, two issues have to be considered, namely *(i)* the competition for irradiance between real water components and DDBQ, and *(ii)* the effect of real water matrices on the DDBQ photodegradation quantum yield.

The ability of natural and treated wastewaters to absorb radiation, which is largely accounted for by the natural organic matter, is usually quantified on the basis of the 254-nm absorbance as the $SUVA_{254nm}$ index (units of L mg$_C^{-1}$ m^{-1}). $SUVA_{254nm}$ is defined as the ratio between the water absorbance at 254 nm over a path length of 1 m and the dissolved organic carbon of the water itself (DOC, units of mg$_C$ L^{-1}). Typical values of $SUVA_{254nm}$ range between 1 and 10 L mg$_C^{-1}$ m^{-1}, while DOC in most cases may reasonably vary between 1 and 20 mg$_C$ L^{-1} (Wetzel, 2001). The $SUVA_{254nm}$ index is very useful in the present case, because it is determined at the same 254-nm wavelength as the emission maximum of the Hg lamps used for the UV_{254} irradiation experiments. One can assume $k^{u.p.}_{DDBQ}$ as the pseudo-first-order photodegradation rate constant of DDBQ in ultra-pure water, and k^W_{DDBQ} as the corresponding DDBQ rate constant in a real water matrix, which is described by the parameters $SUVA_{254nm}$ and DOC. The ratio y between the two rate constants can be

expressed by the following equation, where ε_{DDBQ} (units of $M^{-1}\,m^{-1}$) is referred to 254 nm, b (in meters) is the optical path length, and $C_{o,DDBQ}$ is the substrate concentration:

$$y = \frac{k_{DDBQ}^{u.p.}}{k_{DDBQ}^{W}} = \frac{\Phi_{DDBQ}}{\Phi_{DDBQ}^{a}} \times \frac{\varepsilon_{DDBQ}\,C_{o,DDBQ} + SUVA_{254nm}\,DOC}{\varepsilon_{DDBQ}\,C_{o,DDBQ}} \times \frac{1-\exp(-2.303\varepsilon_{DDBQ}\,b\,C_{o,DDBQ})}{1-\exp[-2.303b(\varepsilon_{DDBQ}\,C_{o,DDBQ} + SUVA_{254nm}\,DOC)]} \quad (6)$$

In most real circumstances the absorbance of DDBQ is expected to be very low, in which case one has $\varepsilon_{DDBQ}\,C_{o,DDBQ} \ll SUVA_{254nm}\,DOC$, as well as $1\text{-}\exp(-2.303\,\varepsilon_{DDBQ}\,b\,C_{o,DDBQ}) \sim 2.303\,\varepsilon_{DDBQ}\,b\,C_{o,DDBQ}$. As a consequence, equation (6) can be simplified as follows:

$$y = \frac{10.2\,SUVA_{254nm}\,b\,DOC}{1-\exp(-2.303\,SUVA_{254nm}\,b\,DOC)} \quad (7)$$

where $10.2 = 2.303\,\Phi_{DDBQ}\,(\Phi_{DDBQ}^{a})^{-1}$. Based on equation (7) and assuming a cm-range value for b ($b = 0.01$ m), it is possible to model the ratio $y = k_{DDBQ}^{u.p.}\,(k_{DDBQ}^{W})^{-1}$ as a function of the possible values of $SUVA_{254nm}$ and DOC. The ratio y is an estimate of how much a laboratory experiment carried out with DDBQ in ultra-pure water would overestimate the DDBQ photodegradation kinetics observed in a real water matrix. The results (see Figure 4a) suggest that laboratory experiments in ultra-pure water could overestimate the DDBQ photodegradation kinetics by up to 20 times, in waters with $SUVA_{254nm} = 10$ L mg_C^{-1} m^{-1} and $DOC = 20$ mg_C L^{-1}. The overestimation would derive from the combination of the $\sim$ 4-fold ratio between Φ_{DDBQ} and Φ_{DDBQ}^{a}, with the competition for lamp irradiance between DDBQ and organic matter.
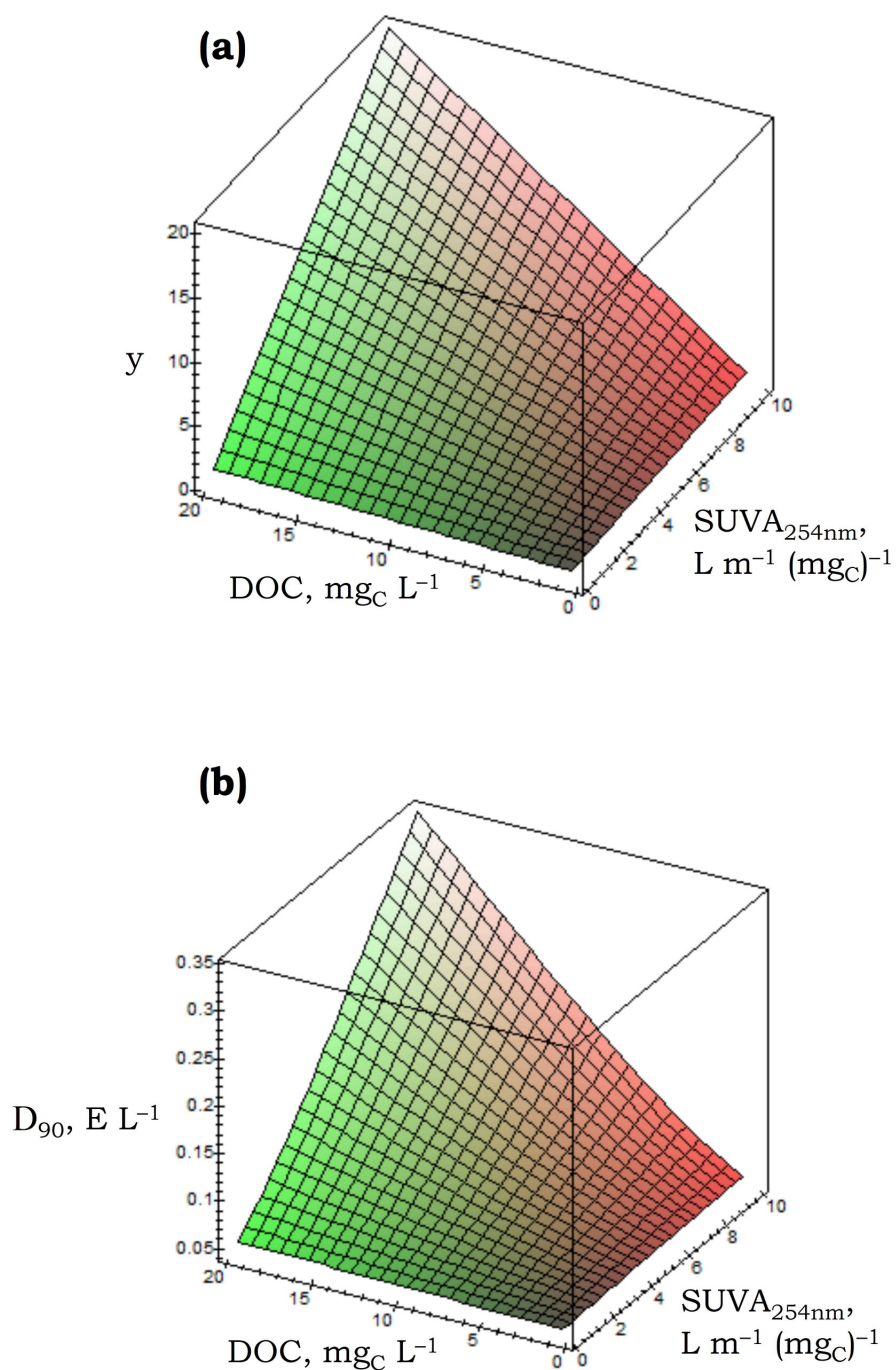
13

Figure 4. Predicted trend of **(a)** the ratio *y* between the DDBQ photodegradation rate constant in ultra-pure water and the rate constant in a real water matrix (see eq. 7), and **(b)** the radiation dose D_{90} required to achieve 90% DDBQ degradation, as a function of the water parameters $SUVA_{254nm}$ and *DOC*. Negligible radiation absorption by DDBQ is assumed here (very low DDBQ concentration). Note that *y* is unit-less. In both cases it was assumed $b = 1$ cm.

Based on the above discussion, one can also assess the UV dose that is necessary to achieve a target degradation of DDBQ, as a function of the water conditions and under the assumption of first-order degradation kinetics. In ultra-pure water, the degradation rate of DDBQ (R_{DDBQ}) depends on radiation absorption and photolysis quantum yield, as follows (I_o is the incident UV light intensity):

$$R^o_{DDBQ} = k^{u.p.}_{DDBQ}\, C_{o,DDBQ} = \Phi_{DDBQ}\, I_o\,[1-\exp(-2.303\,\varepsilon_{DDBQ}\, b\, C_{o,DDBQ})] \qquad (8)$$

If the concentration $C_{o,DDBQ}$ is very low, it is possible to linearize the above equation and obtain the following:

$$k^{u.p.}_{DDBQ} = 2.303\,\Phi_{DDBQ}\, I_o\,\varepsilon_{DDBQ}\, b \qquad (9)$$

In a first-order kinetic framework ($C_{DDBQ} = C_{o,DDBQ}\exp(-k_{DDBQ}\,t)$), a target DDBQ degradation of, say, 90% ($C_{DDBQ}\,(C_{o,DDBQ})^{-1} = 0.1$) would require an input radiation dose $D^{u.p.}_{90} = t^{u.p.}_{90}\, I_o = 2.303\, I_o$ $(k^{u.p.}_{DDBQ})^{-1} = (\Phi_{DDBQ}\,\varepsilon_{DDBQ}\, b)^{-1}$ (note that $t^{u.p.}_{90} = 2.303\,(k^{u.p.}_{DDBQ})^{-1}$, and Eq. (9) was used for the last equation step), which gives $D^{u.p.}_{90} = 0.016$ E L^{-1} if $b = 1$ cm. This dose corresponds to $t^{u.p.}_{90} = 16$ min irradiation time if $I_o = 1.65\times10^{-5}$ E L^{-1} s^{-1} = 9.9×10^{-4} E L^{-1} min^{-1} (same as per our set-up).

Different water matrices would slow down the degradation of DDBQ and, according to Eq. (6), one gets $k^W_{DDBQ} = y^{-1}\, k^{u.p.}_{DDBQ}$. Because $D^W_{90} = 2.303\, I_o\,(k^W_{DDBQ})^{-1}$, the radiation dose D^W_{90} needed to achieve 90% DDBQ degradation would be increased by a factor of y compared to $D^{u.p.}_{90}$. The same would happen to the required treatment time. On this basis, the trend of D_{90} as a function of the water DOC and of $SUVA_{254nm}$ is reported in Figure 4b. The increase of D_{90} with increasing DOC and $SUVA_{254nm}$ is due to radiation screening and Φ_{DDBQ} decrease. Under the worst assumed scenario ($DOC = 20$ mg$_C$ L^{-1}, $SUVA_{254nm} = 10$ L m^{-1} mg$_C^{-1}$) one gets that the needed dose is $D_{90} \sim 0.35$ E L^{-1}, which is around 20 times higher than the dose required in ultra-pure water. However, our worst-case scenario conditions are found in highly colored water that is unlikely to undergo UV$_{254}$ treatment. UV$_{254}$ would rather be applied to extensively pre-treated water where the color intensity is much lower. For instance, in the presence of $DOC = 2$ mgC L^{-1} and $SUVA_{254nm} = 4$ L m^{-1} mg$_C^{-1}$ that produce $A_W = 0.08$ (not far from our studied river water, see Table 1) one gets D$_{90} \sim 0.05$ E L^{-1},

with an increase of about 4 times compared to ultra-pure water. In any case, the application of UV_{254} to natural water matrices has to take into account a significant increase in treatment times compared with experiments in ultra-pure water.

3.2. Transformation products of DDBQ

Exposing aqueous solutions of DDBQ to UV_{254} irradiation afforded the photo-transformation of the parent compound. The chromatograms corresponding to the DAD 285 nm signals for each UV_{254} exposure time are overlaid in Figure S5, visualizing DDBQ degradation and by-product formation as a function of time. Eluting compounds were further analyzed by means of MS. Two of the by-products were tentatively identified as hydroxylated derivatives, where one or both bromine atoms of DDBQ were replaced by OH groups, namely: 2-bromo-3-hydroxyl-5,6-dimethyl-1,4-benzoquinone (OH-BDMBQ) and 2,3-hydroxyl-5,6-dimethyl-1,4-benzoquinone (DOH-DMBQ,). The summary of these investigations is given in Table 2. Identification was based on the distinct isotope patterns found in the ESI mass spectra (Wang et al. 2014, Wang et al. 2016) and previously proposed pathways for HBQs other than the one studied here, where transformation into hydroxylated derivatives was reported to occur (Qian et al. 2013, Wang et al. 2014, Wang et al. 2016). Due to lack of standards of the hydroxylated derivatives, the concentrations of these products could not be determined. The other eluting compounds could not be identified, because the single quadrupole MS used here could only measure ions formed in the instrument's source, resulting in a limited amount of structural information and selectivity.

Figure 5 shows the formation-degradation curves as a function of time for the two photoproducts identified during the photolysis of 50 mg L^{-1} DDBQ in ultra-pure water. Responses (%) were calculated as the percentage of the ratio of the response obtained at each irradiation time over the maximum response recorded for the specific photoproduct. The identified photoproducts pointed towards photoinduced debromination followed by reaction with water to produce the corresponding hydroxylated derivative. A tentative reaction scheme to account for the transformation of DDBQ into the mono-hydroxy derivative is shown in Figure 6. The proposed pathway is based on the ability of C-Br bonds to undergo homolysis under irradiation (Rezende et al., 1995), and on the ease by which hydroxylation reactions may occur in water.
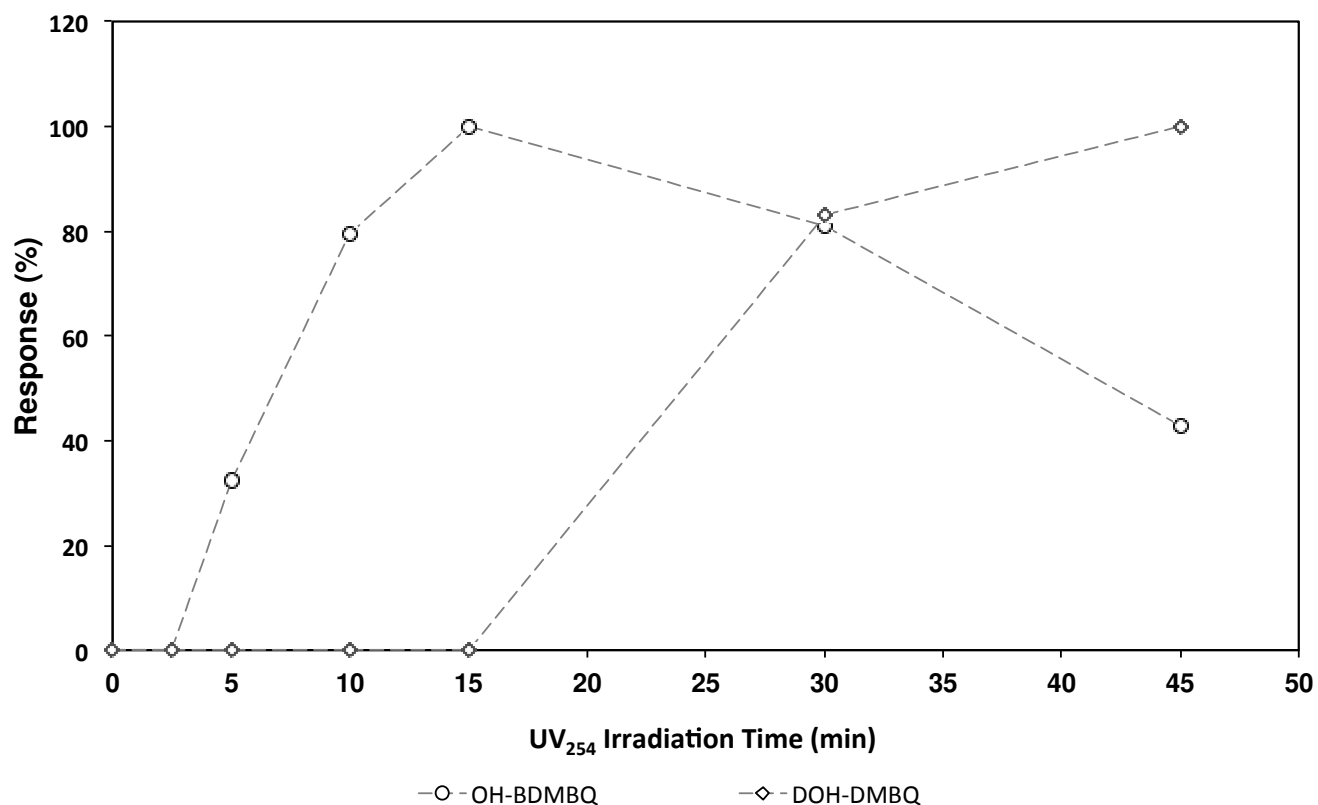
Figure 5. Formation-degradation time profiles of the two photoproducts identified during the UV_{254} photolysis of 50 mg L^{-1} DDBQ in ultra-pure water. Responses (%) represent the percentage ratio of the peak-area at each irradiation time over the maximum response obtained for each photoproduct.
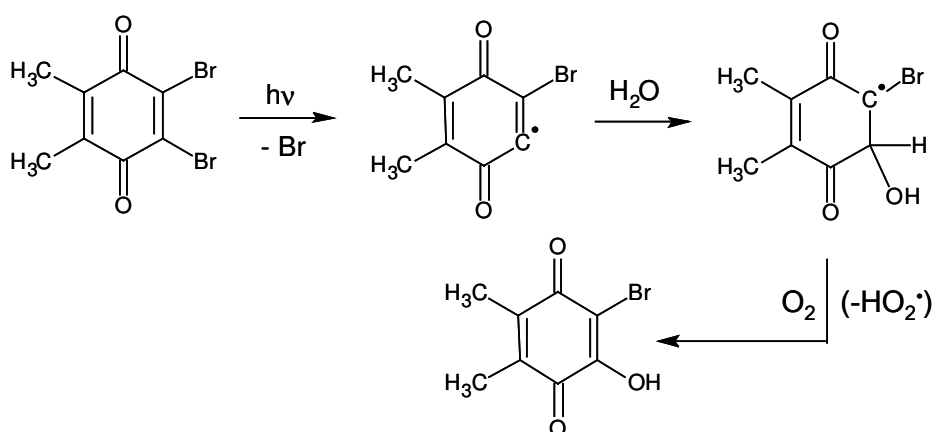

Figure 6. Proposed pathway for the transformation of DDBQ into the monohydroxylated derivative (OH-BDMBQ). An analogous pathway could then yield the dihydroxylated compound.

17

Further insight into the transformation of DDBQ into hydroxylated derivatives was obtained from *in-silico* toxicity estimates carried out by using the ECOSAR software. DDBQ is a quinone and, as such, it is particularly toxic to fish and algae: it is expected to show acute toxicity at sub-ppm levels, and chronic toxicity at ppb levels. The two hydroxylated derivatives are expected to be about as toxic as DDBQ (see Table S2), except that DOH-DMBQ is predicted to be less chronically toxic than DDBQ towards crustaceans. Therefore, the transformation of DDBQ into OH-BDMBQ and DOH-BDMBQ would not lead to real detoxification, at least as far as the considered toxicity endpoints are concerned. Although this may not be a point of concern for OH-BDMBQ, which is relatively well degraded, DOH-BDMBQ was found to accumulate with irradiation time. A closer examination of Figure 5 shows that DOH-BDMBQ was still undetectable when OH-BDMBQ reached its maximum concentration, and the decrease of OH-BDMBQ after the maximum occurred together with DOH-BDMBQ accumulation. As a compromise, an irradiation time in the range of 30-45 min under the present experimental conditions (i.e., those of Figure 5) would enable >90% DDBQ degradation and different degrees of OH-BDMBQ decrease and DOH-BDMBQ accumulation. A more precise assessment would require the availability of real standards to assess the concentrations of the hydroxyderivatives and their formation yields from DDBQ.

4. Conclusions

The disinfection by-product DDBQ can be degraded with the UV_{254} treatment, and the process is enabled by the fairly high absorption coefficient of this compound at 254 nm (3380 M^{-1} cm^{-1}). The photodegradation kinetics does not depend on pH, but it is affected by humic acids and by components that occur in both natural waters and treated wastewater. In addition to screening light, interfering substances are able to decrease the DDBQ photolysis quantum yield, from the value of 0.018 observed in ultra-pure water to 0.004-0.005. Because of the combination of light screening and quantum yield decrease, the photodegradation of DDBQ in natural water matrices would be significantly slower than in ultra-pure water. This has implications for the radiation dose that is required to reach a given treatment target, and should be taken into account when planning the UV_{254} treatment of DDBQ. This contribution provides a numerical approach by which to foresee the extent of degradation inhibition, on the basis of the $SUVA_{254nm}$ and DOC values of treated water.

The phototransformation of DDBQ yields hydroxyderivatives, most likely via a debromination-hydroxylation pathway. *In-silico* toxicity screening suggests that the transformation of DDBQ into the detected hydroxyderivatives would not eliminate toxicity, but the monohydroxylated derivative (OH-BDMBQ) undergoes rather fast transformation that would limit the associated problems. In contrast, the dihydroxylated compound (DOH-BDMBQ) was found to accumulate during irradiation. Due to the different time trends, it would be difficult to find conditions that minimize the occurrence of DDBQ and both products. However, it is possible to find irradiation conditions where DDBQ degradation exceeds 90%, OH-BDMBQ starts decreasing after the maximum, and the accumulation of DOH-BDMBQ is still limited. It might not be convenient to prolong irradiation much further, because of DOH-BDMBQ accumulation and cost considerations.

The present results provide evidence that photolytical conversion of DDBQ occurs and is a fast process. However, it is acknowledged that it is difficult to extrapolate these results to real-life scenarios, as well as reach general conclusions for the studied water matrices. The protocol adopted here used an artificial light source and the composition of the studied real matrices may differ from others found on site. From this perspective, our experiment might appear optimal and we agree that extrapolations from laboratory measurements may result in significant under-prediction of photolysis lifetime. Nevertheless, the present findings suggest that phototransformation of DDBQ may be an important transformation mechanism, and the timescale in which it occurs makes UV_{254} treatment an interesting process to consider.

5. References

Anichina, J., Zhao, Y., Hrudey, S.E., Le, X.C., Li, X.-F., 2010. Electrospray ionization mass spectrometry characterization of interactions of newly identified water disinfection byproducts halobenzoquinones with oligodeoxynucleotides. Environ. Sci. Technol. 44, 9557–9563. DOI:10.1021/es1024492

Beltran, F.J., Ovejero, G., García-Araya, J.F., Rivast, J., 1995. Oxidation of polynuclear aromatic hydrocarbons in water. 2. UV radiation and ozonation in the presence of UV radiation. Ind. Eng. Chem. Res. 34, 1607–1615. DOI: 10.1021/ie00044a013

Braslavsky, S.E., 2007. Glossary of terms used in photochemistry, 3rd edition. Pure Appl. Chem. 79, 293-465.

Bull, R.J., Reckhow, D.A., Li, X., Humpaged A.R, Joll C., Hrudey, S.E., 2011. Potential carcinogenic hazards of non-regulated disinfection by-products: Haloquinones, halo-cyclopentene and cyclohexene derivatives, N-halamines, halonitriles, and heterocyclic amines. Toxicology 286, 1- 19. DOI:10.1016/j.tox.2011.05.004

Canonica, S., Laubscher, H.-U., 2008. Inhibitory effect of dissolved organic matter on triplet-induced oxidation of aquatic contaminants. Photochem. Photobiol. Sci. 7, 547-551. DOI: 10.1039/B719982A

Chu, L., Anastasio, C., 2005. Formation of hydroxyl radical from the photolysis of frozen hydrogen peroxide. J. Phys. Chem. A, 109, 6264-6271. DOI:10.1021/jp051415f

Fang, J., Fu, Y., Shang, C., 2014. The roles of reactive species in micropollutant degradation in the UV/free chlorine system. Environ. Sci. Technol., 48, 1859–1868. DOI: 10.1021/es4036094

Frank, R. A., Sanderson, H., Kavanagh, R., Burnison, B. K., Headley, J. V., Solomon, K. R., 2010. Use of a (quantitative) structure–activity relationship [(Q)Sar] model to predict the toxicity of naphthenic acids. J. Toxicol. Env. Heal. A 73, 319 – 329. DOI: 10.1080/15287390903421235

Garoma, T., Gurol, M.D., 2005. Modeling aqueous ozone/UV process using oxalic acid as probe chemical. Environ. Sci. Technol., 39, 7964-7969. DOI: 10.1021/es050878w

Gligorovski, S., Strekowski, R., Barbati S., Vione, D. 2015. Environmental implications of hydroxyl radicals ($^\bullet$OH). Chem. Rev., 115, 13051-13092. DOI: 10.1021/cr500310b

Görrer, H., 2003. Photoprocesses of p-benzoquinones in aqueous solution. J. Phys. Chem. A 107, 11587-11595. DOI: 10.1021/jp030789a

Javier Benitez, F., Acero, J. L., Real, F. J., Roldan, G., Rodriguez, E., 2013. Photolysis of model emerging contaminants in ultra-pure water: Kinetics, by-products formation and degradation pathways. Water Res. 47, 870-880. DOI: 10.1016/j.watres.2012.11.016

Lanzafame, G. M., Sarakha, M., Fabbri, D., Vione, D. 2017. Degradation of methyl 2-aminobenzoate (methyl anthranilate) by H_2O_2/UV: Effect of inorganic anions and derived radicals. Molecules22, article n. 619. DOI: 10.3390/molecules22040619

Li, J., Wang, W., Moe, B., Wang, H., Li, X.-F., 2015. Chemical and toxicological characterization of halobenzoquinones, an emerging class of disinfection byproducts. Chem. Res. Toxicol. 28, 306−318. DOI: 10.1021/tx500494r

Mayo-Bean, K., Moran, K., Meylan, B., Ranslow, P., 2012. Methodology document for the ECOlogical Structure-Activity Relationship model (ECOSAR) class program. US-EPA, Washington DC, 46 pp.

Nicole, I., De Laat, J., Dore, M., Duguet J.P., Bonnel, C., 1990. Use of UV radiation in water treatment: Measurement of photonic flux by hydrogen peroxide actinometry. Water Res. 2, 157-168. DOI: 10.1016/0043-1354(90)90098-Q

Ortiz de García, S.A., Pinto Pinto, G., García-Encina, P.A., Irusta-Mata, R., 2014. Ecotoxicity and environmental risk assessment of pharmaceuticals and personal care products in aquatic environments and wastewater treatment plants. Ecotoxicology 23, 1517-1533. DOI: 10.1007/s10646-014-1293-8

Qian, Y., Wang, W., Boyd, J. M., Wu, M., Hrudey, S. E., & Li, X. F., 2013. UV-induced transformation of four halobenzoquinones in drinking water. Environ. Sci. Technol. 47, 4426–4433. DOI:10.1021/es305044k

Qin, F.; Zhao, Y.-Y.; Zhao, Y.; Boyd, J. M.; Zhou, W.; Li, X.-F., 2010. A Toxic Disinfection By-product, 2,6-Dichloro-1,4-benzoquinone, Identified in Drinking Water. Angew. Chem., Int. Ed. 49, 790-792. DOI:10.1002/anie.200904934

Reuschenbach, P., Silvani, M., Dammann, M., Warnecke, D., Knacker, T., 2008. ECOSAR model performance with a large test set of industrial chemicals. Chemosphere 71, 1986-1995. DOI: 10.1016/j.chemosphere.2007.12.006.

Rezende, D. D., Campos, I. P. D., Toscano, V. G., Catalani, L. H., 1995. Photolysis of a series of alpha-brominated ortho-xylenes in apolar solvents. J. Chem. Soc. Perkin Trans. II 10, 1857-1862.

Sarr, D.H., Kazunga, C., Charles, M.J., Pavlovich, J.G., Aitken, M.D., 1995. Decomposition of tetrachloro-1,4-benzoquinone (p-chloranil) in aqueous-solution. Environ. Sci. Technol. 29, 2735–2740. DOI: 0013-936X/95/0929-2735

Schwarzenbach, R.P., Gschwend, P.M., Imboden, D.M., 2003. Environmental Organic Chemistry, second ed., John Wiley & Sons, New York.

Veltsistas, P.G., Karayannis, M.I., Koupparis, M.A., 1994. Potentiometric determination of p-chloranil and the kinetic-study of its alkaline-hydrolysis, using a chloranilate selective electrode. Talanta 41 1725–1733. DOI: 10.1016/0039-9140(94)E0114-7.

Vione D., Khanra S., Das R., Minero C., Maurino V., Brigante M., Mailhot G., 2010. Effect of dissolved organic compounds on the photodegradation of the herbicide MCPA in aqueous solution. Water Res. 44, 6053-6062. DOI: 10.1016/j.watres.2010.07.079

Wang, W., Qian, Y. Boyd, J.M., Wu, M., Hrudey, S.E., Li, X.F., 2013, Halobenzoquinones in swimming pool waters and their formation from personal care products. Environ. Sci. Technol. 47, 3275-3282. DOI: 10.1021/es304938x

Wang, W., Qian, Y., Li, J., Moe, B., Huang, R., Zhang, H., Li, X.-F., 2014. Analytical and toxicity characterization of halo-hydroxyl-benzoquinones as stable halobenzoquinone disinfection byproducts in treated water. Anal. Chem. 86, 4982–4988. DOI:10.1021/ac5007238

Wang, W., Moe, B., Li, J., Qian, Y., Zheng, Q., Li, X.-F., 2016. Analytical characterization, occurrence, transformation, and removal of the emerging disinfection byproducts halobenzoquinones in water. Trends Analyt. Chem. 85, 97–110. DOI:10.1016/j.trac.2016.03.004

Wetzel, R. G., 2001. Limnology of lake and river ecosystems, 3rd edn., Academic Press, New York.

Zhao, Y., Qin, F., Boyd, J. M., Anichina, J., Li, X. F., 2010. Characterization and determination of chloro- and bromo-benzoquinones as new chlorination disinfection byproducts in drinking water. Anal. Chem. 82, 4599–4605. DOI:10.1021/ac100708u

Zhao, Y., Anichina, J., Lu, X., Bull, R. J., Krasner, S. W., Hrudey, S. E., Li, X. F., 2012. Occurrence and formation of chloro- and bromobenzoquinones during drinking water disinfection. Water Res. 46, 4351-60. DOI: 10.1016/j.watres.2012.05.032

Table 1. Spectral features of the studied natural and treated wastewater matrices (A_W is the water absorbance in the used photoreactor device), as well as the ratios between the absorbed photon fluxes (ρ, see Eq. (5)) and the experimental degradation rate constants ($\rho' = k_{DDBQ\,alone}(k_{DDBQ,W})^{-1}$) of DDBQ in ultra-pure and real water. The apparent quantum yield of DDBQ photodegradation in real water (Φ^a_{DDBQ}) is also reported.

Matrix	A_W	ρ	ρ'	Φ^a_{DDBQ}
River water	0.09	1.07	4.73	0.0040
Seawater	0.12	1.09	4.81	0.0040
Wastewater	0.16	1.11	4.45	0.0044

Table 2. Degradation products obtained during the UV$_{254}$ photolysis of DDBQ in ultra-pure water. DDBQ eluted at 19.5 min in the MS and the identification ion had m/z = 294 amu.

Product	DAD Retention time (min)[a]	MS Retention time (min)[b]	Identification ion (amu)	Tentative identification
By-product 1	13.1	13.3	229	**OH-BDMBQ**
By-product 2	6.1	6.3	165	**DOH-DMBQ**

[a] DAD signal at 285 nm

[b] MS signal; negative ESI